Gamma-Ray Induced Radiation Damage in Large Size LSO and LYSO Crystal Samples

Jianming Chen, *Member, IEEE*, Rihua Mao, *Member, IEEE*, Liyuan Zhang, *Member, IEEE*, and Ren-yuan Zhu, *Senior Member, IEEE*

***Abstract*—This paper presents a study of the gamma-ray induced radiation damage effect in large size ($2.5 \times 2.5 \times 20\ \mathrm{cm}^3$) LSO and LYSO crystal samples. Optical and scintillation properties, including longitudinal transmittance and photo-luminescence spectra, light output and light response uniformity with PMT and APD readout, are measured before and after γ-ray irradiations with an integrated dose up to 10^6 rad for three LSO and LYSO samples from different vendors. It was found that 300°C thermal annealing removes all radiation induced absorption. The photo-luminescence spectra measured before and after the irradiations were found to be consistent, indicating that the scintillation mechanism is not damaged. The radiation damage recovers very slow under the room temperature, indicating that the radiation damage level in LSO and LYSO crystals is not dose rate dependent. It was also found that the overall radiation damage in LSO and LYSO crystals is small as compared to other crystal scintillators commonly used in high energy and nuclear physics experiments.**

***Index Terms*—Crystal, light output, lutetium oxyorthosilicate, lutetium yttrium oxyorthosilicate, photo-luminescence, radiation damage, scintillator, transmission.**

I. Introduction

FOLLOWING our previous studies [1], [2] this report presents a further study on radiation damage in large size lutetium oxyorthosilicate (Lu_2SiO_5, LSO) [3] and lutetium-yttrium oxyorthosilicate ($Lu_{2(1-x)}Y_{2x}SiO_5$, LYSO) [4], [5] crystals. Because of their high stopping power ($X_0 = 1.14$ cm, $R_{Moliere} = 2.07$ cm) and fast ($\tau = \sim 40$ ns) bright (4 times of BGO) scintillation, LSO and LYSO crystals have attracted a broad interest in the high energy physics community for future experiments, such as a super B factory [6] and the international linear collider (ILC) [7].

Fig. 1 is a photo showing three long crystal samples with a dimension of $2.5 \times 2.5 \times 20$ cm. They are, from top to bottom, an LYSO sample from Crystal Photonics, Inc. (CPI), an LYSO sample from Saint-Gobain Ceramics & Plastics, Inc. (Saint-Gobain) and an LSO sample from CTI Molecular Imaging (CTI). It is noted that the CPI LYSO sample has chips at the corners and surfaces since CPI does not have adequate polishing and treatment facilities for such large size samples [8]. These long LSO and LYSO samples were specially prepared by manufactures for the authors.

Manuscript received December 15, 2006; revised April 19, 2007. This work was supported in part by the U.S. Department of Energy Grant DE-FG03-92-ER40701.

The authors are with the California Institute of Technology, Pasadena, CA 91125 USA (e-mail: zhu@hep.caltech.edu).

Color versions of one or more of the figures in this paper are available online at http://ieeexplore.ieee.org.

Digital Object Identifier 10.1109/TNS.2007.902370

Measurements for LYSO crystal samples of such size with PMT readout were reported in [1]. Results for LSO and LYSO crystal samples of such size with both PMT and APD readout were reported in [2]. γ-ray induced radiation damage was investigated by several authors for LSO samples of up to a few centimeter long [9]–[11]. To judge the feasibility of these crystal's potential applications in an radiation environment, however, measurements must be made on full size crystal samples. This is due to the fact that crystal's light output is affected by both its scintillation yield, which may be investigated by using small samples, and the light propagation inside the crystal, which can only be studied by using full size samples. In addition, it is well known that defect control is more difficult for large size crystals than selected small samples.

According to the manufacturers, the yttrium content is about 5% for the CPI LYSO [8] and about 10% for the Saint-Gobain LYSO [12]. The nominal cerium doping level is 0.2% for the CTI LSO [13] and the CPI LYSO [8], and is less than 1% for the Saint-Gobain LYSO [12]. The details of crystal manufacturing, such as the seed or the tail end during the growth process, are not provided by the manufacturers. All surfaces of these samples are polished. A thermal annealing at 300°C for 10 hours was applied to all samples prior to the irradiations. As discussed below this process removes all γ-ray induced absorption.

γ-ray irradiations were carried out at two irradiation facilities at Caltech: an open 50 curie ^{60}Co source and a closed 2,000 curie ^{137}Cs source. The former provides dose rates of 2 and 100 rad/h by placing samples at appropriate distances. The later provides a dose rate of 8,500 rad/h with 5% uniformity along sample's longitudinal axis when samples are placed at the center of the irradiation chamber. A series of irradiations was carried out step by step with integrated doses of 10, 10^2, 10^3, 10^4, 10^5 and 10^6 rad. Table I lists the integrated dose, the dose rate applied to these samples and the corresponding irradiation time for each step. Optical and scintillation properties, including longitudinal transmittance and photo-luminescence spectra, light output and light response uniformity with photomultiplier (PMT) and avalanche photodiode (APD) readout, were measured before and 24 hours after each step of the irradiations. Samples were kept in the dark at the room temperature during the entire experiment to avoid any thermal annealing and optical bleaching.

II. Damage in Scintillation and Optical Properties

A. Photo-Luminescence

Samples were first irradiated at a dose rate of 8,500 rad/h for 96 hours. Excitation and photo-luminescence spectra were mea-

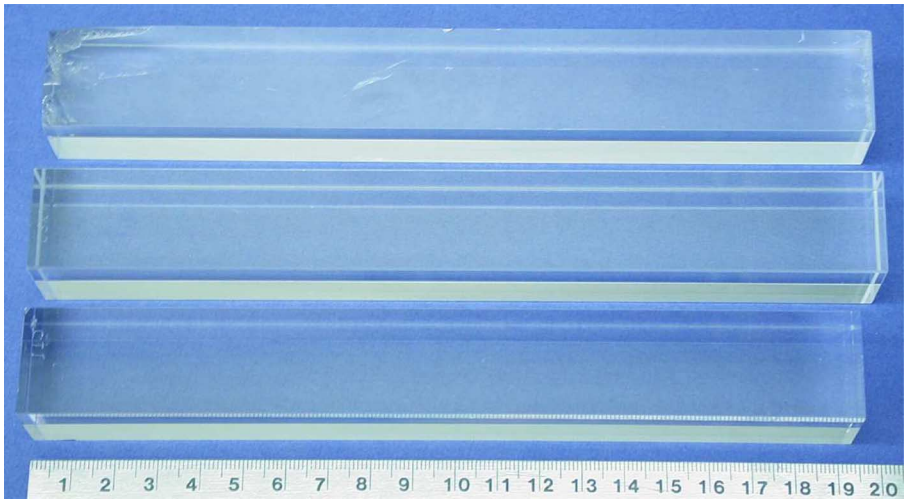

Fig. 1. A photo showing three long (2.5 × 2.5 × 20 cm) crystal samples, from top to bottom: CPI LYSO, SG LYSO and CTI LSO.

TABLE I
IRRADIATION TIME AND THE INTEGRATED DOSE

Dose (rad)	10	10^2	10^3	10^4	10^5	10^6
γ-ray Source	^{60}Co	^{60}Co	^{137}Cs	^{137}Cs	^{137}Cs	^{137}Cs
Dose rate (rad/h)	2	100	8,500	8,500	8,500	8,500
Time (hour)	5	0.9	0.106	1.06	10.6	100.6

sured using a Hitachi F-4500 fluorescence spectrophotometer before and after the irradiation. For the excitation and photo-luminescence spectra, a UV excitation light was shot to a bare surface of the sample, and the crystal was oriented so that the photo-luminescence light is not affected by sample's internal absorption. The top plot of Fig. 2 shows the photo-luminescence spectra of the SG-LYSO sample measured before (solid) and after (dashes) the irradiation. To facilitate a comparison these spectra were normalized to the area between 380 and 460 nm under the spectra. The corresponding relative difference is shown in the bottom plot of Fig. 2. The bin by bin average of the absolute difference between the spectra measured before and after the irradiation is found to be 0.6% in the normalization region, less than the $\sim 1\%$ systematic uncertainty. This indicates that the γ-ray irradiation does not affect the scintillation mechanism in LSO and LYSO crystals.

B. Recovery of the Longitudinal Transmittance

Transmittance spectra were measured by a Perkin Elmer Lambda-950 UV/Vis/NIR spectrophotometer with double beam, double monochromator and an optical bench for these long samples before and after each irradiation step. The systematic uncertainty in repeated measurements is about 0.15%.

Fig. 3 shows the measured longitudinal transmittance values at 420 nm as a function of the time after the 96 hour irradiation at a dose rate of 8,500 rad/h, where T_0 is the transmittance measured before the irradiation. Although the T_0 values are different for these samples because of different surface conditions, the overal amplitude of radiation damage in the longitudinal transmittanceis is observed to be about 10% for all three

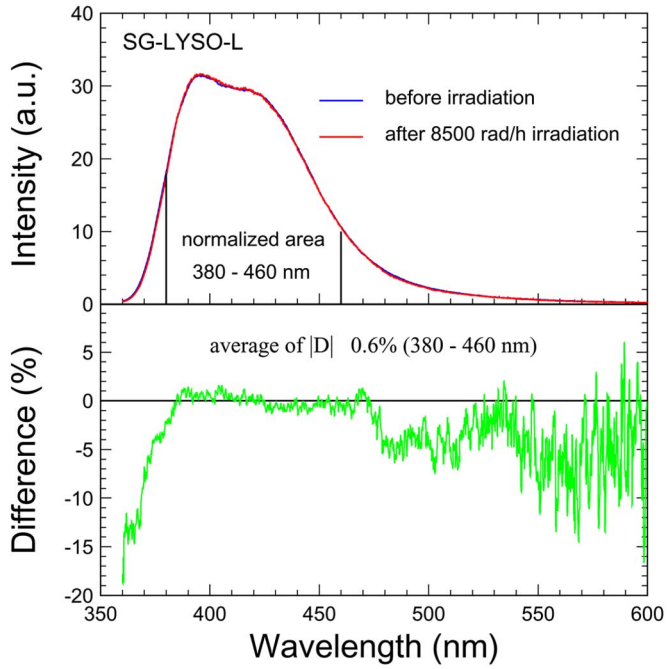

Fig. 2. Top: Photo-luminescence spectra are shown as a function of wavelength for samples SG-LYSO before (solid) and after (dashes) irradiation. Bottom: The corresponding difference of these spectra is shown as a function of wavelength.

samples after this irradiation. Data for each sample are fit to a linear function of time after the irradiation. The slopes were found to be $(8 \pm 5) \times 10^{-4}\%h^{-1}$, $(2 \pm 2) \times 10^{-4}\%h^{-1}$ and $(0 \pm 2) \times 10^{-4}\%h^{-1}$ respectively for samples CPI, CTI and Saint-Gobain. The observed radiation damage recovery thus is

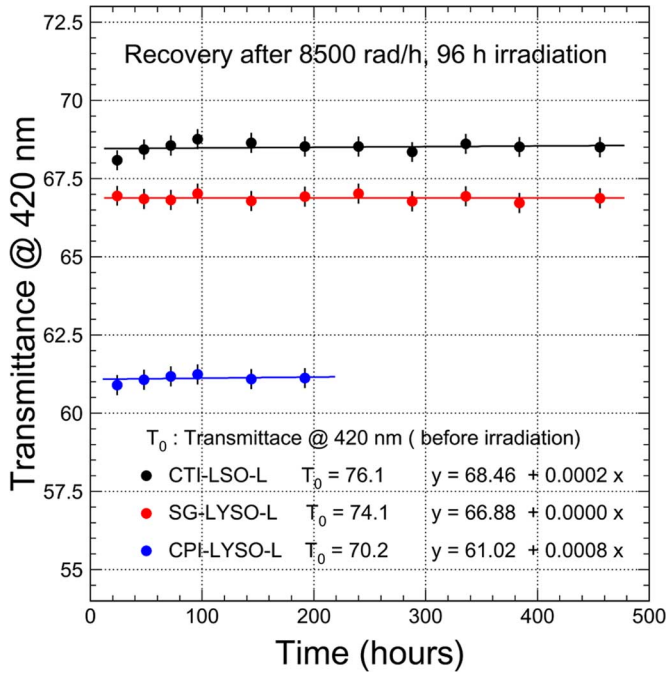

Fig. 3. Values of the longitudinal transmittance at 420 nm are shown as a function of time for samples CTI-LSO, CPI-LYSO and SG-LYSO after a 96 hour irradiation at 8,500 rad/h.

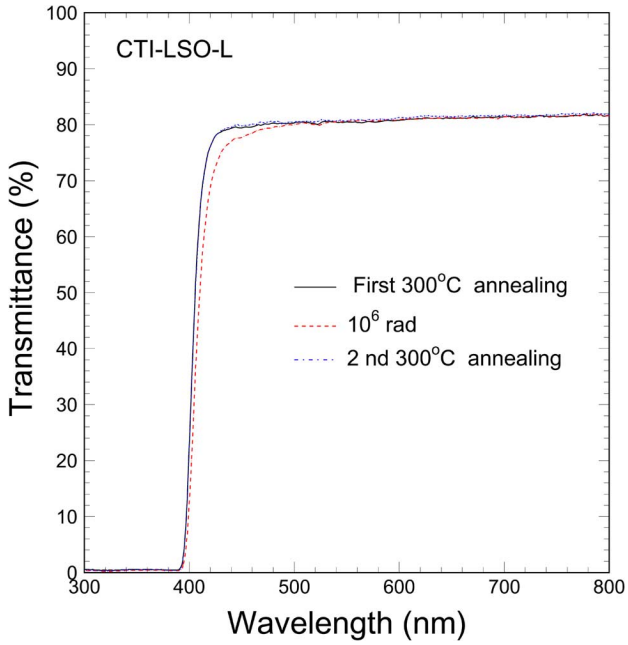

Fig. 4. The longitudinal transmittance spectra are shown as a function of wavelength for CTI-LSO sample measured after the first 300°C thermal annealing, after an irradiation with integrated dose of 10^6 rad and after the second 300°C thermal annealing.

very slow for the LSO and LYSO samples under the room temperature, indicating that the radiation damage effect in LSO and LYSO crystals is not dose rate dependent [14].

C. Thermal Annealing and Transmittance Damage

All samples were annealed at 300°C for 10 hours before going through the series of irradiations. This thermal annealing was found to be effective in eliminating the radiation induced absorption in the LSO and LYSO samples. Fig. 4 shows three longitudinal transmittance spectra measured for the CTI-LSO sample after the 1st thermal annealing at 300°C, after the irradiations with cumulated γ-ray dose of 10^6 rad and after the 2nd thermal annealing at 300°C. While the overall amplitude of the radiation damage in the longitudinal transmittance is small (about 10% at 420 nm) it was completely eliminated after the 2nd thermal annealing.

After thermal annealing, samples were irradiated step by step to integrated doses of 10, 10^2, 10^3, 10^4, 10^5 and 10^6 rad, as shown in Table I. Integrated dose is used to present the level of the radiation applied in this study since radiation damage in LSO and LYSO crystals is not dose rate dependent. Fig. 5 shows an expanded view of the longitudinal transmittance spectra for these samples before and after several steps of the γ-ray irradiations with integrated dose of 10^2, 10^4 and 10^6 rad. Also shown in the figure is the corresponding numerical values of the photo-luminescence weighted longitudinal transmittance (*EWLT*), which is defined as

$$EWLT = \frac{\int LT(\lambda)Em(\lambda)d\lambda}{\int Em(\lambda)d\lambda}. \quad (1)$$

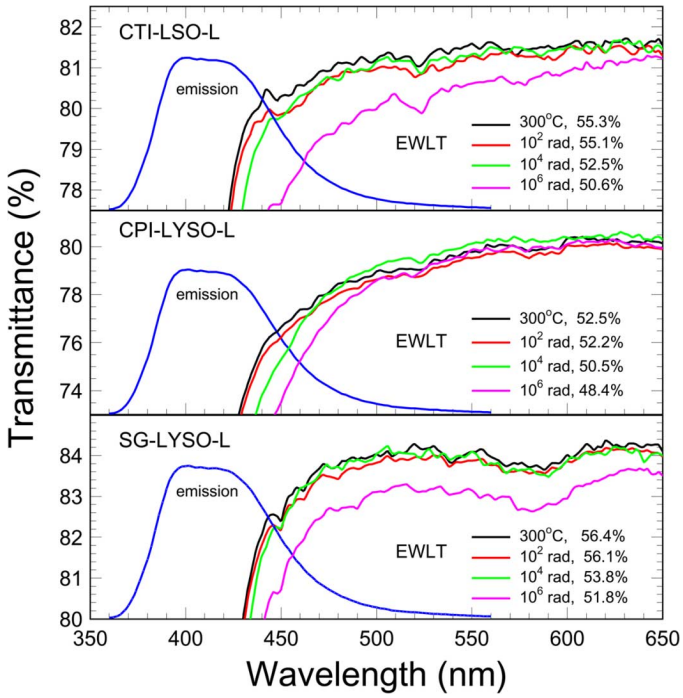

Fig. 5. The transmittance spectra are shown as a function of wavelength in an expanded scale together with the photo-luminescence spectra for CTI-LSO, CPI-LYSO and SG-LYSO samples before and after the irradiations with integrated doses of 10^2, 10^4 and 10^6 rad.

A continuous degradation of transmittance was observed. This observation differs from our previous observation [1], where a slight increase of transmittance was observed during a low dose irradiation. That increase may be caused by the existing residual absorption in these samples before the irradiations since they were not thermally annealed before the irradiations. These

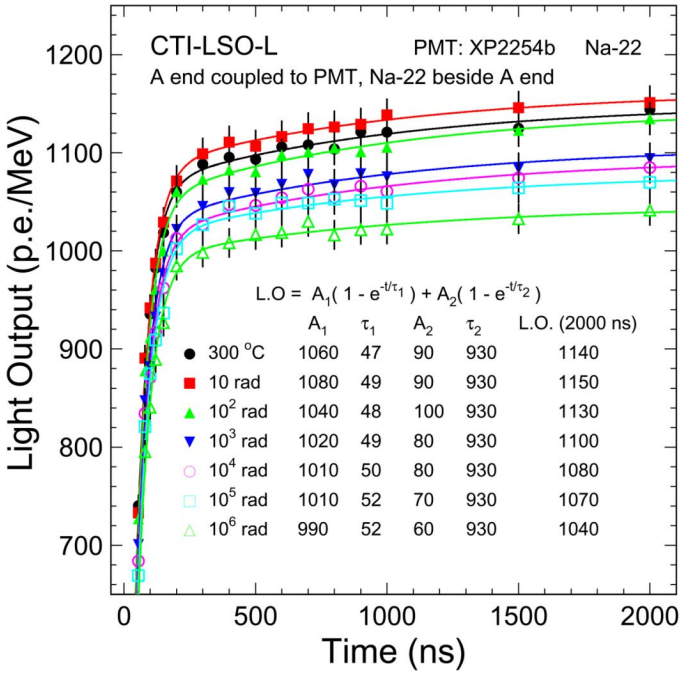

Fig. 6. Light output measured by using the XP2254b PMT is shown as a function of the integration time for the CTI-LSO sample before and after the series of irradiations with various integrated doses.

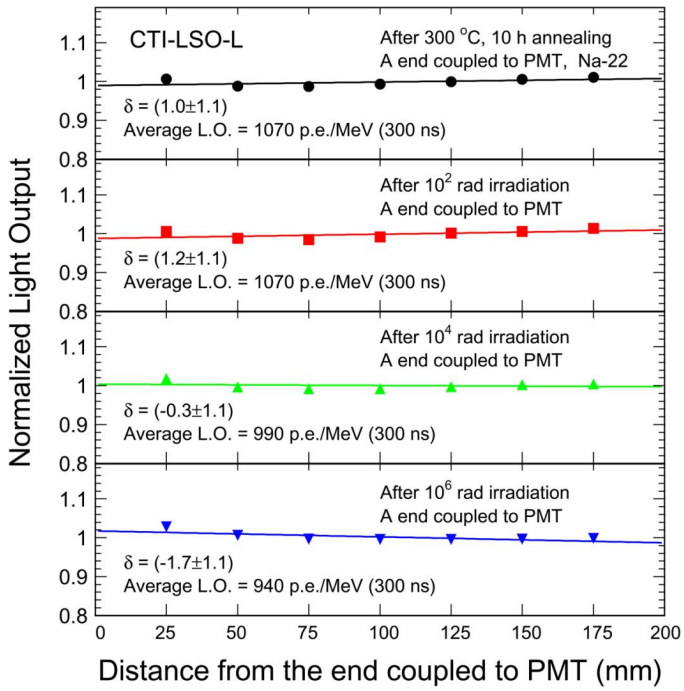

Fig. 7. Light response uniformities are shown for the CTI-LSO sample with the A end coupled to the XP2254b PMT before and after the irradiations with integrated doses of 10^2, 10^4 and 10^6.

residual absorptions were optically self-bleached by the scintillation light in our previous study. No difference was observed between LSO and LYSO samples in this measurement.

The relative degradation of EWLT is 8.5%, 7.8% and 8.2% respectively for CTI-LSO, CPI-LYSO and SG-LYSO after the final step of an integrated dose of 10^6 rad. This amplitude of the observed *EWLT* variations is smaller than crystal scintillators commonly used in experimental physics [14], indicating that LSO and LYSO crystals are more radiation resistant.

III. Light Output and Response Uniformity With the PMT Readout

The light output and decay kinetics were measured using a Photonis XP2254b PMT, which has a multi-alkali photo cathode and a quartz window. To reduce the effect of the intrinsic natural radioactivity, a collimated $^{22}\mathrm{Na}$ source was used with a coincidence trigger provided by a $\mathrm{BaF_2}$ crystal. The set-up used in this measurement can be found in [2]. The γ-ray peak position was obtained by a simple Gaussian fit. In these measurements one end of the sample was coupled to the readout device with Dow corning 200 fluid, while all other faces of the sample were wrapped with Tyvek paper.

Since we can not distinguish the seed end from the tail end, the A end was define such that the sample produces a lower light when it was coupled to the PMT. The other end is defined as the B end. Fig. 6 shows light output as a function of integration time for CTI-LSO before and after the irradiations with the A end coupled to the PMT. The corresponding fits for two decay components are also shown in the figure. Although there is a degradation in the light output no change in the decay kinetics was observed.

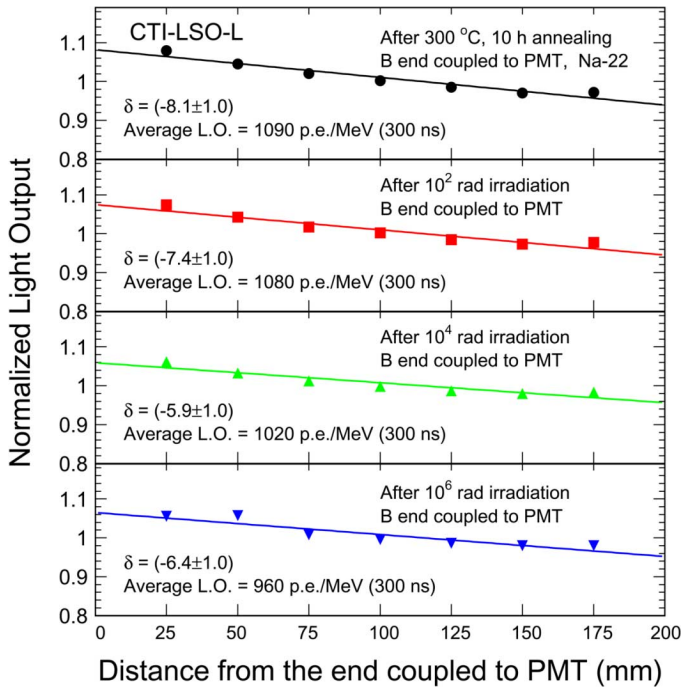

Fig. 8. The same as Fig. 7 with the B end coupled to the XP2254b PMT.

The light response uniformity was measured for long samples by shooting a collimated $^{22}\mathrm{Na}$ γ-ray source at seven evenly distributed locations along crystal's longitudinal axis with coincidence trigger. The responses at these seven points were fit to a linear function, Figs. 7 and 8 show light response uniformity for

TABLE II
RESULT OF LIGHT OUTPUT AND LIGHT RESPONSE UNIFORMITY WITH PMT READOUT

Sample ID	Integrated dose (rad)	A end coupled		B end coupled	
		LO^*_{mid}	δ (%)	LO^*_{mid}	δ (%)
CTI-LSO	annealing	1070	1±1	1090	-8±1
	10	1080	1±1	1100	-8±1
	10^2	1070	1±1	1080	-7±1
	10^3	1030	1±1	1050	-7±1
	10^4	990	0±1	1020	-6±1
	10^5	980	-1±1	1000	-6±1
	10^6	940	-2±1	960	-6±1
CPI-LYSO	annealing	950	1±1	990	-5±1
	10	970	0±1	1000	-4±1
	10^2	950	0±1	980	-4±1
	10^3	940	0±1	930	-5±1
	10^4	910	0±1	920	-5±1
	10^5	870	-1±1	870	-3±1
	10^6	850	-2±1	850	-3±1
SG-LYSO	annealing	1090	0±1	1090	-5±1
	10	1090	-1±1	1090	-5±1
	10^2	1080	-1±1	1080	-6±1
	10^3	1050	-1±1	1070	-5±1
	10^4	1010	0±1	1040	-6±1
	10^5	940	0±1	970	-6±1
	10^6	920	0±1	950	-5±1

* LO_{mid}: light output at the middle of the sample (p.e./MeV).

the CTI-LSO sample with the A end and the B end coupled to the PMT respectively.

$$\frac{LO}{LO_{mid}} = 1 + \delta\left(\frac{x}{x_{mid} - 1}\right) \tag{2}$$

where LO_{mid} represents the average light output at the middle of the sample, δ represents the deviation of the light response uniformity, and x is the distance from the end coupled to the readout device.

Table II summarizes the numerical values of the light response uniformity measurements. The δ values are different for the A end and the B end coupled to the PMT. This observation is consistent with our previous observation [1]. It is well known that the light output of these cerium doped crystals is affected by the cerium concentration [13] as well as the yttrium fraction in LYSO samples [8]. Any longitudinal variation in the Ce concentration would affect long sample's light response uniformity. Effort will have to be made to develop long crystals of consistent light response uniformity under irradiations [14].

Fig. 9 shows the degradation of the normalized average light output, LO_{mid}, with the A end (top) and the B end (bottom) coupled to the PMT for all three samples after each step of irradiations. With the A end coupled to the PMT, the degradation in the average light output after the 10^6 rad irradiation is 12%, 11% and 16% respectively for CIT-LSO, CPI-LYSO and SG-LYSO, while it is 12%, 14% and 13% for the B end coupled to the PMT.

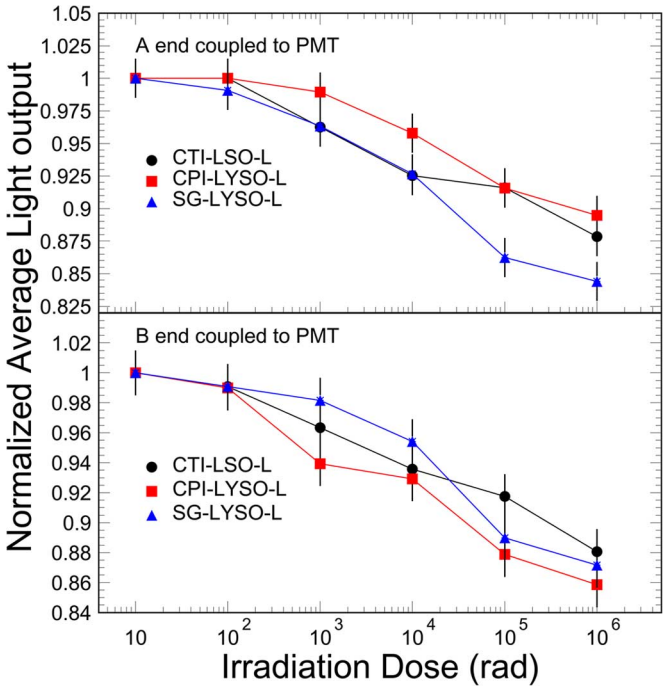

Fig. 9. Normalized light output with A (top) and B (bottom) end coupled to the XP2254b PMT is shown as a function of the integration dose for the CTI-LSO, CPI-LYSO and SG-LYSO samples.

IV. Light Output and Response Uniformity With the APD Readout

Magnetic field excludes the use of PMT as the readout device in most high energy physics experiments. Solid state devices, such as silicon photodiode (PD) or avalanche photodiode (APD), are usually used since they are immune to magnetic field. Because of lacking sufficient amplification, the use of the solid state readout would lead to a large readout noise. For crystals with low light output, laboratory measurements are often done with PMT. Because of their high light output, however, the light output of LSO and LYSO crystals may also be measured by silicon APDs in laboratory using conventional radioactive source.

Two commercial available Hamamatsu S8664-55 APDs are used as the readout device for the APD readout, which has a dimension of 5×5 mm. The total readout area is 0.5 cm^2, corresponding to 8% coverage of crystal's back face. This low coverage was more or less compensated by the 75% quantum efficiency for LSO and LYSO scintillation light [2]. To reduce systematic uncertainties the APDs were glued to a quartz plate which then coupled to the crystals through Dow corning 200 fluid. They were reverse biased at 400 V with corresponding gain about 50. Their output went through a Canberra 2003 BT preamplifier and an ORTEC 673 shaping amplifier with shaping time set at 250 ns. To reduce the effect of the intrinsic natural radioactivity, a collimated $^{22}\mathrm{Na}$ source was used with a coincidence trigger provided by a BaF_2 crystal. The detailed description of the set-up used for the APD readout can be found in [2].

Fig. 10 shows spectra of 0.511 MeV γ-rays from a $^{22}\mathrm{Na}$ source measured with S8664-55 APDs with coincidence trigger for the CTI-LSO sample. Clear γ-ray peaks are visible for the sample even after an integrated dose of 10^6 rad. Figs. 11 and 12 show the light response uniformities measured by S8664-55 APDs with 0.511 MeV γ-rays from a $^{22}\mathrm{Na}$ source and a coincidence trigger for the CTI-LSO sample with the A end and the B end coupled to the APDs respectively.

Table III summarizes the numerical results. Comparing with the result obtained with the PMT readout, a larger difference between the δ values is observed between the ends coupled to the readout device. Since the PMT readout covers 100% of the back face while the APD readout covers only 8%, the average path lengths for the scintillation light to reach the readout devices are very different for these two readout devices. A rigorous ray-tracing simulation would help to understand the nature of this difference [14].

Once again, we observed the coupling end dependent uniformity slopes δ and a minor degradation of the average light output. Fig. 13 shows the corresponding degradations of the average light output measured with the A end (top) and the B end (bottom) coupled to the S8664-55 APDs for all three samples. With the A end coupled to the APDs, the degradation in light output after the 10^6 rad irradiation is 12%, 9% and 10% respectively for CIT-LSO, CPI-LYSO and SG-LYSO, while it is 12%, 11% and 10% for the B end coupled to the APDs.

V. Summary

Three long LSO and LYSO crystal samples have gone through a series γ-ray irradiations with an integrated dose of up to 10^6 rad. It was found that the shape of the photo-luminescence spectra are not affected by the γ-ray irradiations, indicating that there is no damage in the scintillation mechanism. It was also found that 300°C thermal annealing removes all γ-ray induced absorption. The recovery under the room

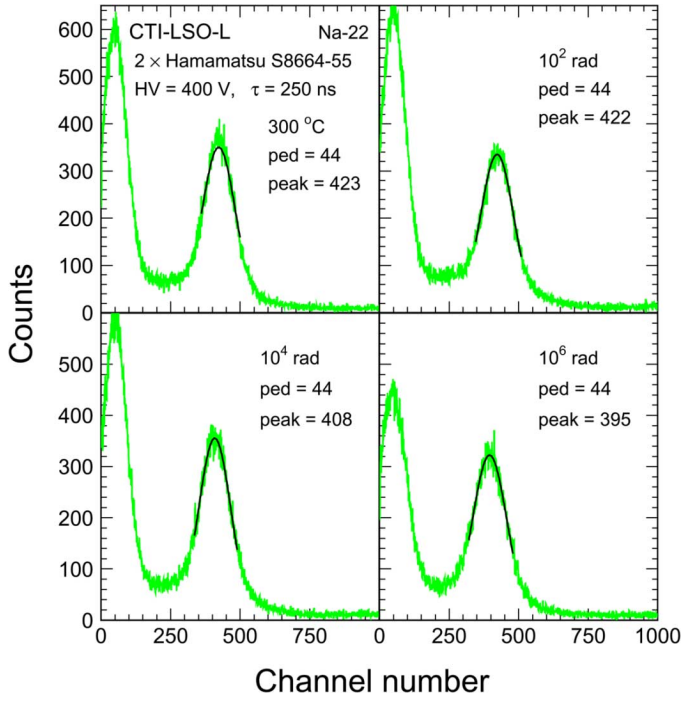

Fig. 10. The spectra of 0.511 MeV γ-rays from a $^{22}\mathrm{Na}$ source measured using two Hamamatsu S8664-55 APD with coincidence trigger are shown for the CTI-LSO sample before and after the irradiations with integrated doses of 10^2, 10^4 and 10^6 rad.

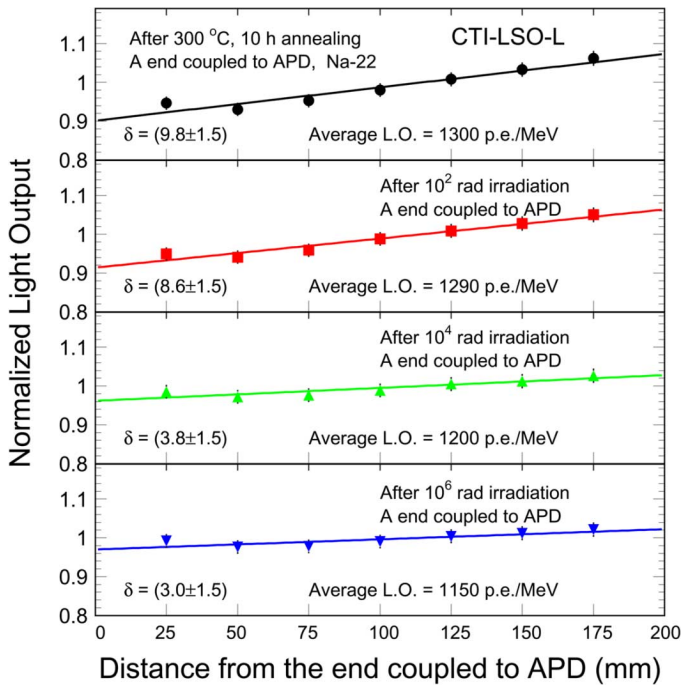

Fig. 11. Light response uniformities are shown for the CTI-LSO sample with the A end coupled to the S8664-55 APDs before and after the irradiations with integrated doses of 10^2, 10^4 and 10^6.

TABLE III
RESULT OF LIGHT OUTPUT AND LIGHT RESPONSE UNIFORMITY WITH APD READOUT

Sample ID	Integrated dose (rad)	A end coupled		B end coupled	
		LO^*_{mid}	δ (%)	LO^*_{mid}	δ (%)
CTI-LSO	annealing	1300	10±1.5	1310	-11±1.5
	10	1310	9±1.5	1300	-10±1.5
	10^2	1290	9±1.5	1270	-10±1.5
	10^3	1240	6±1.5	1250	-9±1.5
	10^4	1200	4±1.5	1220	-6±1.5
	10^5	1190	4±1.5	1210	-5±1.5
	10^6	1150	3±1.5	1150	-7±1.5
CPI-LYSO	annealing	980	7±1.5	1030	-1±1.5
	10	1000	8±1.5	1030	-1±1.5
	10^2	1000	8±1.5	1010	-1±1.5
	10^3	950	7±1.5	980	1±1.5
	10^4	940	7±1.5	950	0±1.5
	10^5	930	7±1.5	950	1±1.5
	10^6	890	5±1.5	920	0±1.5
SG-LYSO	annealing	1120	8±1.5	1110	-5±1.5
	10	1120	7±1.5	1110	-5±1.5
	10^2	1120	7±1.5	1090	-5±1.5
	10^3	1110	7±1.5	1080	-5±1.5
	10^4	1070	7±1.5	1070	-6±1.5
	10^5	1040	7±1.5	1010	-7±1.5
	10^6	1010	6±1.5	1000	-6±1.5

* LO_{mid}: light output at the middle of the sample (p.e./MeV).

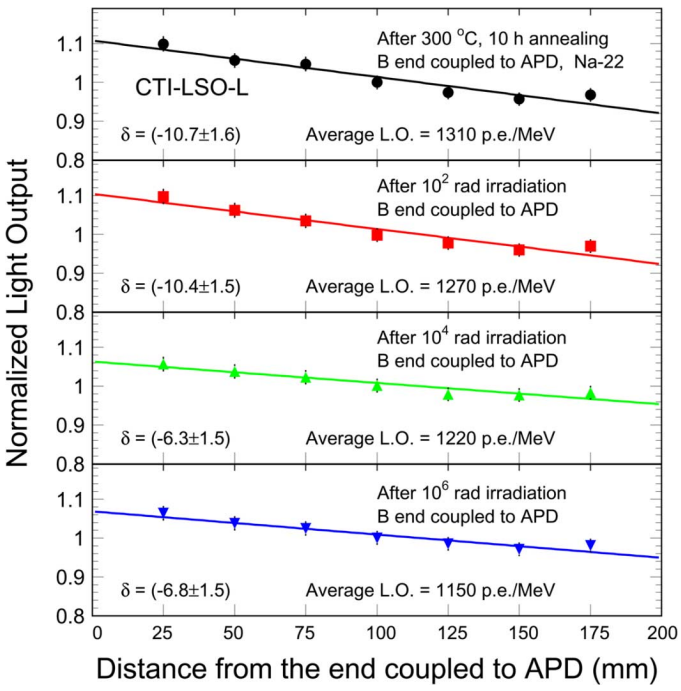

Fig. 12. The same as Fig. 11 with the B end coupled to the APD for the CTI-LSO sample.

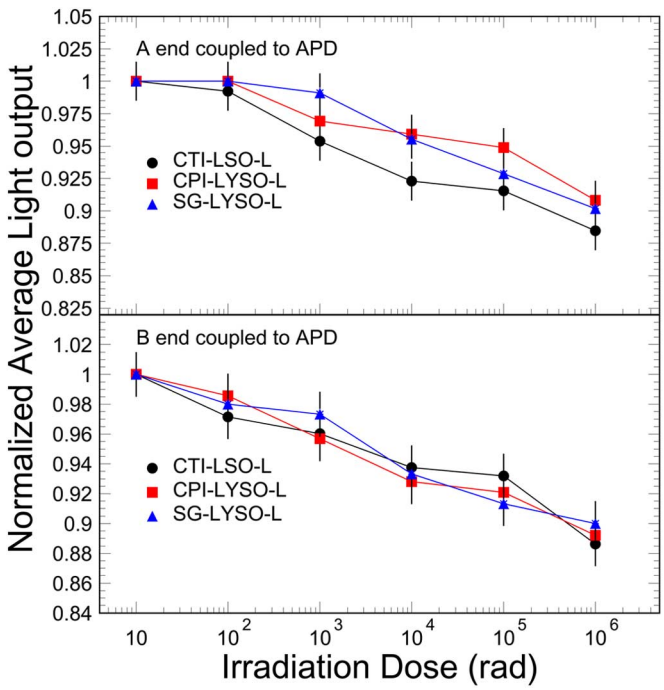

Fig. 13. Normalized light output with A (top) and B (bottom) end coupled to the S8664-55 APDs is shown as a function of the integration dose for the CTI-LSO, CPI-LYSO and SG-LYSO samples.

temperature is found to be very slow for all samples after the irradiations, indicating that the radiation damage in LSO and LYSO crystals is not dose rate dependent. Typical light output loss measured by both PMT and APD readout is found to be at 12% level for these samples after the γ-ray irradiations with an integrated dose of 10^6rad. The overall radiation damage effect

in the LSO and LYSO crystals thus is small as compared to other commonly used crystal scintillators. In a brief summary, LSO and LYSO crystals are a good candidate for a precision crystal calorimeter in high energy and nuclear physics experiments.

ACKNOWLEDGMENT

The authors would like to thank Dr. B. Chai, Dr. C. Melcher, and Dr. D. Rothan for many useful discussions.

REFERENCES

[1] J. M. Chen, L. Y. Zhang, and R. Y. Zhu, "Large size LYSO crystals for future high energy physics experiments," *IEEE Trans. Nucl. Sci.*, vol. 52, no. 6, pp. 2133–3140, Dec. 2005.

[2] J. M. Chen, R. H. Mao, L. Y. Zhang, and R. Y. Zhu, "Large Size LSO and LYSO Crystals for Future High Energy Physics Experiments," *IEEE Trans. Nucl. Sci.*, vol. 54, no. 3, pp. 718–724, Jun. 2007.

[3] C. Melcher and J. Schweitzer, "Cerium-doped lutetium oxyorthosilicate: A fast, efficient new scintillator," *IEEE Trans. Nucl. Sci.*, vol. 39, no. 4, pp. 502–505, Aug. 1992.

[4] D. W. Cooke, K. J. McClellan, B. L. Bennett, J. M. Roper, M. T. Whittaker, and R. E. Muenchausen, "Crystal growth and optical characterization of cerium-doped $\mathrm{Lu_{1.8}Y_{0.2}SiO_5}$," *J. Appl. Phys.*, vol. 88, pp. 7360–7362, 2000.

[5] T. Kimble, M. Chou, and B. H. T. Chai, "Scintillation properties of LYSO crystals," in *Proc. IEEE Nuclear Science Symp. Conf.*, Nov. 2002, pp. 1434–1437.

[6] W. Wisniewski, R. Zhu, Ed., "Consideration for calorimetry at a super B factory," in *Proc. 10th Int. Conf. Calorimetry in Particle Physics*, Pasadena, CA, Mar. 2002.

[7] R.-Y. Zhu, "An LSO/LYSO crystal calorimeter for the ILC," in *Proc. Int. Linear Collider Physics and Detector Workshop, 2nd ILC Accelerator Workshop*, Snowmass, CO, Aug. 2005, pp. 14–27.

[8] B. Chai, private communication.

[9] L. Qin, Y. Pei, S. Lu, Z. Yin, and G. H. Ren, "A new radiation damage phenomenon of LSO:Ce scintillation crystal," *Nucl. Instrum. Methods Phys. Res. A*, vol. A545, pp. 273–277, 2005.

[10] P. Kozma and P. Kozma, Jr, "Radiation sensitivity of GSO and LSO scintillator detectors," *Nucl. Instrum. Methods Phys. Res. A*, vol. A539, pp. 132–136, 2004.

[11] M. Kobayashi, M. Ishii, and C. L. Melcher, "Radiation damage of a cerium-doped lutetium oxyorthosilicate single crystal," *Nucl. Instrum. Methods Phys. Res. A*, vol. A335, pp. 509–512, 1993.

[12] D. Rothan, private communication.

[13] C. Melcher, private communication.

[14] R.-Y. Zhu, "Radiation damage in scintillating crystals," *Nucl. Instrum. Methods Phys. Res. A*, vol. A413, pp. 297–311, 1998.